

***Ficus Religiosa* Bark an Efficient Adsorbent for Alizarin Red S dye: Equilibrium and Kinetic Analysis**

Ammara Gul¹, Sayyar Muhammad*¹, Saleem Nawaz¹, Sidra Munir¹, Khushnood Ur Rehman², Saeed Ahmad³ & Olivier S. Humphrey⁴

¹*Department of Chemistry, Islamia College Peshawar, 25120-Peshawar Khyber-Pakhtunkhwa, Pakistan*

²*Department of Botany, Islamia College Peshawar, 25120-Peshawar Khyber-Pakhtunkhwa, Pakistan*

³*Division of Agricultural and Environmental Sciences, School of Biosciences, University of Nottingham, Sutton Bonnington Campus, Loughborough, Leicestershire LE12 5RD, United Kingdom*

⁴*Centre for Environmental Geochemistry, Inorganic Geochemistry, British Geological Survey, Nottingham NG12 5GG, United Kingdom*

**Corresponding author:*

e-mail: sayyar@icp.edu.pk

ORCID: 0000-0001-6282-9750

Phone: +92-3339724809

Abstract

The discharge of unsafe colour dyes into the effluents of various industries can harm the environment and human health and therefore needs remediation. The current research assesses the environmental friendly decontamination of the Alizarin Red S (ARS) dye from industrial aqueous effluents by powder bark of a low-cost and indigenous plant, *Ficus religiosa*, as a biosorbent. The biosorbent was processed, powdered, and then characterized via SEM and FTIR spectroscopy before and after exposure to ARS. For maximum dye-decontamination of industrial effluents, adsorption parameters including dosage of the biosorbent, contact time between the dye and the biosorbent, shaking time and temperature of the adsorption process were optimized. SEM images confirmed the presence of high surface area active binding sites and FTIR analysis shows that the adsorption of ARS on the adsorbent is due to groups like –OH, –NH, –CH, C=O and C=C. The kinetics study of the adsorption follows pseudo-second order kinetic model. Best fit isotherm to the equilibrium data was obtained for Langmuir and Freundlich models. The decontamination ARS from aqueous phase by the adsorption process could be an inexpensive and viable way of protecting humans from carcinogenicity, DNA mutagenicity, jaundices, allergies and skin irritations.

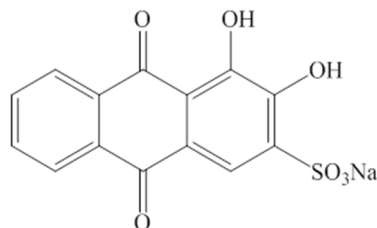
Keywords: Adsorption isotherm; Alizarin Red S; *Ficus religiosa*; Equilibrium; Kinetic; Wastewater treatment

Introduction

Pollution caused by the discharge of effluents from industry, agriculture and other sources in to the inland water resources such as rivers, canals and lakes can cause adverse effects on human and aquatic life [1-3]. Water contaminated with dyes is one of the major sources of environmental pollution [4]. Dyes are mostly organic compounds that are used extensively in various industries such as dyeing, textile, pulp and printing. Due to abundant utilization of water in these industries and discharge of wastewater in high volume could constitute a problem for the environment, as the wastewater has potentially significant concentrations of dissolved dyes. Most of the dyes are highly stable and non-biodegradable because of their synthetic origin and complex aromatic

structures [5]. The presence of these colorants in aquatic ecosystems restrict sunlight from penetrating the water body significantly inhibiting native flora and fauna [4, 6-7]. Dye-polluted water can cause cancer, jaundice, DNA mutations, allergies and skin irritation in humans [5, 8-10].

Alizarin Red S (a salt of sodium with 1, 2-dihydroxy-9, 10-anthraquinone sulfonic acid) having chemical formula $C_{14}H_7NaO_7S$ (structure formula shown below) and belongs to anthraquinone dye type.



Alizarin Red S

It is soluble in water and is mainly employed in textile industries as ARS can effectively color wool, cotton and silk without the aid of auxiliary binding agents [11]. Apart from the textile industry, ARS is also used as an indicator in an acid-base titration, determination of fluorine, staining and polishing [12]. Recently biochemical analyses revealed that ARS dye is one of the major pollutants from the textile industry which is long-lasting and not easily manageable [13]. It causes nephritis, malformation and mutagenicity in humans and can damage the aquatic environment [14-16].

One of the most important areas of the research involving water pollution control is the removal of dyes from industrial effluents. A variety of treatment techniques including filtration [17], ion-exchange [18], coagulation/flocculation [19], electrolysis [20], reverse osmosis [21], waste water treatment by non-noble metal/reduced graphene oxide nanocomposite coated on wood and wood-based double-layer photo-absorbers [22-23], wastewater treatment by advance oxidation processes [24], adsorption are used for discoloring of wastewater [25-27]. Most of these processes are not cost-effective. The most successful, inexpensive and productive process for dyes removal from aqueous industrial contaminants is the adsorption phenomenon [28]. The adsorption of dye on a cheap, reusable and nontoxic adsorbent with a high surface area can eliminate a higher proportion (up to 99%) of pollutant dye from wastewater and give high-grade clean water [29].

The use of the biosorption technique in dyed wastewater treatment has earned considerable attention due to its operational simplicity, flexibility and technical feasibility [6]. A wide variety of inexpensive and effective biosorbents are reported in the literature which has shown excellent efficacy. Chitosan, plant biomass, roots, stem, bark and leaves of trees as well as agricultural wastes, are the most common and cheaper biosorbent materials used for effective elimination of dyes from various effluents worldwide [1, 6, 30-35]. *Ficus religiosa* or sacred fig, locally known as peepal tree, is a widely recognized common medicinal plant with excellent adsorption capacity [36]. ARS decontamination is performed on using a variety of adsorbent including chickpea husk [12], mustard husk [37], *Cyanodon dactylon* [38], *Lantana camara* [39] and activated charcoal [40]. Rao et al. has employed the powdered leaves of *Ficus religiosa* for adsorption of cadmium from aqueous solutions [35]. However, as far as we know the powdered bark of *Ficus religiosa* has not been utilized as an adsorbent for the adsorptive removal of ARS. This study is the first investigation to report the use of *Ficus religiosa* bark powder as a biosorbent for removal and de-colorations of ARS dye contaminated wastewater. Therefore, the current study aimed to use the powder bark of a common and indigenously available medicinal plant, *Ficus religiosa*, as a

biosorbent for the decontamination of ARS loaded industrial water effluents by a simple and eco-friendly analytical technique. For this assessment, the bark of *Ficus religiosa* was fabricated, chemically modified, characterized through SEM analysis and FTIR spectroscopy. Batch experiments were performed for optimization of maximum adsorption capacity of the biosorbent for the dye.

Materials and Method

Collection and chemical modification of biosorbent

The bark was collected from *Ficus religiosa* plant available in the botanical garden of the Islamia College Peshawar, Pakistan. After collection, samples were triple washed with distilled water and then oven dried. The dried biosorbent was crushed with an electric grinder and sieved to < 250 μm particle size. The fine powder was treated with 0.1 M H_2SO_4 (98%) solution for 24 hours then filtered and finally washed with distilled water several times for excess acid removal. The treated bark powder was finally vacuum filtered and then oven dried.

Characterization of biosorbent by SEM and FTIR

Scanning electron microscopy images can help in the determination of morphology and surface properties including particle size, shape and porosity of biosorbent [41]. The biosorbent was characterized for its composition/morphology using SEM (JEOL JSM-5910, Japan), before and after the chemical modification and the results obtained are discussed below in the results and discussion section.

Fourier transformation infrared (FTIR) spectroscopy is an important analytical technique that gives information about both quantitative and qualitative identification of materials [42]. The information about functional groups that were responsible for the adsorption of the dye on the biosorbent surface was obtained by subjecting the biosorbent sample, before and after the adsorption of the dye, to FTIR spectrometer (IR Prestige-21, FTIR-8400, Shimadzu, Japan, 4000 to 400 cm^{-1}).

Preparation of ARS solution

A 400 mg L^{-1} stock solution was obtained by adding 0.2 g of ARS in doubled distilled water and made the final volume to 500 mL in a flask. From the stock solution 5, 10, 15 and 20 mg L^{-1} initial concentrations of ARS dye were prepared by dilution method.

Batch biosorption experiments

The adsorption of ARS onto the powdered bark of *Ficus religiosa* and the influence of different parameters including the biosorbent dose, initial concentration of the dye, shaking and time of contact between the adsorbent and the dye and temperature was carried out.

Determination of optimum adsorbent dose

The adsorption capacity of a biosorbent can be strongly affected by the amount of biosorbent used in the analysis. For this purpose, 0.25, 0.50, 0.75, and 1.0 g of the biosorbent was weighted by an analytical balance (ATX 224, Shimadzu, Japan) and taken in separate 100 mL flasks containing 5, 10, 15 and 20 mg L^{-1} ARS solutions. The capacity of adsorption of the adsorbent was determined at an optimum contact time of 16 hours at 25 °C. The data was obtained in triplicate and the error bar was ± 0.05 for individual samples.

Effect of shaking and contact times

The mechanical shaker (orbital mechanical shaker KJ-201BS, Oscillator, South Korea) was set at 30, 45 and 60 minutes at 120 rpm for each of the above ARS solutions at 25 °C and 16 hours equilibrium contact time. For study the influence of the adsorbent dose, 0.50 g of the adsorbent was taken in each sample solution of ARS. The influence of contact time between the biosorbent and the ARS dye on the biosorption process in 5, 10, 15 and 20

mg L⁻¹ of 100 mL ARS, at contact times 8, 16, 24, 32 and 40 hours were used at 30 minutes shaking time and 25 °C.

Influence of temperature on adsorption

The temperature of the adsorbate solution can also drastically affect the rate of adsorption process. For different dye solution, the influence of temperature is different but generally, most of the dyes shows high removal capacity at higher temperatures. Temperature effect on the adsorption equilibrium was studied at 15, 25, 35 and 45 °C keeping the adsorbent dose 0.50 g, shaking time 30 minutes and contact time 16 hours.

UV-Visible analysis

The residual concentration of ARS dye was determined by spectroscopic analysis using UV-visible analyser (adsorption Optima sp-300 spectrophotometer, Japan) at the characteristic wavelength of 520 nm at which maximum absorbance occur. The values of the residual concentrations were obtained by interpolation using the calibration curve for the dye solution concentration versus absorbance. The adsorption capacity of the biosorbent was determined from Eq. 1 [1, 28, 41-42].

$$Q_e = \frac{(C_o - C_e)V}{m} \quad (1)$$

Here Q_e represents the quantity of ARS adsorbed on the quantity of the biosorbent at equilibrium in mg g⁻¹ is called also the adsorption capacity, C_o the starting ARS solutions concentration in mg L⁻¹, C_e the concentration at equilibrium of ARS solutions in mg L⁻¹, V the ARS solution volume in L and m the adsorbent mass in g.

Kinetic study

Different kinetic models can be employed to biosorption systems for the equilibrium modelling and determining the mass transfer and reaction mechanism of adsorption. Adsorption properties, experimental and physiochemical conditions can drastically influence the kinetic models [45]. For kinetic study of the adsorption of ARS onto *Ficus religiosa* bark powder, the equilibrium data was tested on pseudo 1st order (Eqn. 2) and 2nd order (Eqn. 3) kinetic equations [46-47].

$$\log(Q_e - Q_t) = \log Q_e - \frac{k_1}{2.303} t \quad (2)$$

$$\frac{t}{Q_t} = \frac{1}{k_2 Q_e^2} + \frac{t}{Q_e} \quad (3)$$

Where, Q_t is the quantity of ARS adsorbed at time t . The values of rate constants for the pseudo 1st order Eqn. (k_1) and 2nd order Eqn. (k_2) can be obtained from the slope of the plots. The results were obtained in triplicate and the replicates were generally within $\pm 5\%$ for individual samples.

Adsorption isotherm models

The data was applied to Langmuir model, Freundlich model and Tempkin adsorption model and the results obtained are discussed. These Isotherms helped in finding the relationship between adsorption capacity of adsorbent and equilibrium concentration. The linear equations of the three isotherm models are given by Eqn. 4 (Langmuir model), Eqn. 5 (Freundlich model) and model Eqn. 6 (Tempkin model), respectively [38, 46].

$$\frac{1}{Q_e} = \left(\frac{1}{K_L Q_{max}} \right) \left(\frac{1}{C_e} \right) + \left(\frac{1}{Q_{max}} \right) \quad (4)$$

$$\log Q_e = \frac{1}{n} \log C_e + \log K_F \quad (5)$$

$$Q_e = K_T \ln C_e + b_T \quad (6)$$

Where, Q_e is the equilibrium capacity of adsorption, C_e is the adsorbate concentration at equilibrium, Freundlich constant n represents adsorption intensity and K_F adsorption capacity, respectively. Langmuir constants Q_{max} .

represents maximum monolayer adsorption capacity in mg g^{-1} and K_L the affinity of the binding sites in L mg^{-1} . K_T and b_T (KJ mol^{-1}) are constants for Temkin isotherm. b_T represents the adsorption potential of the adsorbent.

Results and discussion

SEM micrographs of the adsorbent

Figure 1 indicates the SEM micrographs of the biosorbent before treatment (Fig. 1a), after treatment with H_2SO_4 (Fig. 1b) and after exposure to ARS dye (Fig. 1c). The SEM image (Fig. 1a) revealed that the surface of the *Ficus religiosa* adsorbent was irregular, heterogeneous, and having porous surface with various cavities before it was treated with H_2SO_4 . The number of cavities and active sites of different pore sizes increase and become more visible after the adsorbent treatment with H_2SO_4 (Fig. 1b). The active sites can help in the adsorption of dye. The more the number of active sites available, more could be the chances of dye adsorption on to the adsorbent surface. SEM image of the adsorbent loaded with the ARS dye (Fig. 1c) shows that all the binding sites on the biosorbent are occupied by the dye molecules.

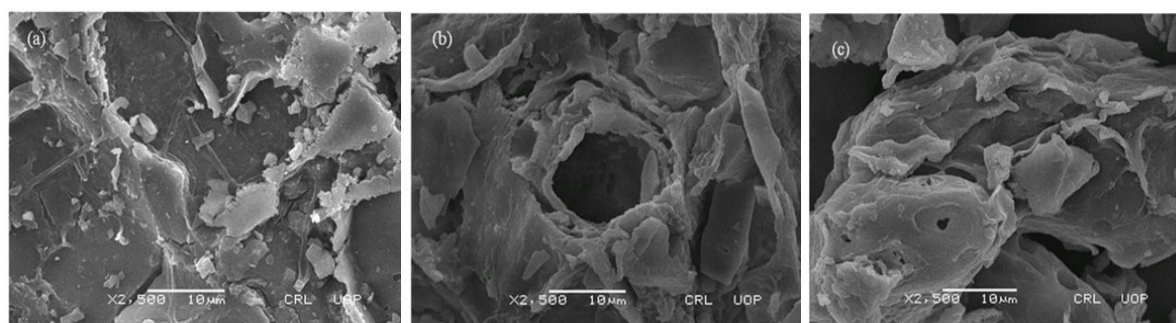


Fig. 1 SEM images of *Ficus religiosa* (a) before treatment with acid, (b) after treatment with H_2SO_4 and (c) after loaded with Alizarin Red S dye.

FTIR spectral analysis

The FTIR spectra of biosorbent obtained in 4000 to 400 cm^{-1} range, before and after ARS dye adsorption (Fig. 2a and 2b). The wavelength range from 1500 - 400 cm^{-1} is attributed to fingerprint region and 4000 - 1500 cm^{-1} to the functional group region [42]. Spectra of the *Ficus religiosa* bark powder adsorbent obtained prior to ARS dye adsorption (Fig. 2a) indicates the absorption bands in 3500 - 3100 cm^{-1} corresponds to the hydroxyl, $-\text{OH}$ functional groups [43] and 3100 - 2900 cm^{-1} to $-\text{CH}$ stretching vibrations and in 2900 - 2600 cm^{-1} corresponds to $-\text{NH}$ stretching vibration. The absorption bands in the range from 1800 - 1500 cm^{-1} are due to functional groups, $\text{C}=\text{O}$ and $\text{C}=\text{C}$ bending vibrations (Jawad & Abdulhameed, 2020). Where bending vibration bands for $\text{C}-\text{C}$, $\text{C}=\text{O}$ and $\text{N}-\text{H}$ occurs at 1500 - 1000 cm^{-1} as evident from Fig. 2a.

The spectra shown in Fig. 2b was taken after the dye adsorption on to pores on the surface of the adsorbent. If we compare Fig. 2b with the FTIR spectra before ARS adsorption onto the adsorbent surface (Fig. 2a), it is clear that the depth for adsorption bands at each of the functional group has decreased as these functional groups are masked by the dye adsorption. For example, the $-\text{OH}$ and $-\text{CH}$ stretching absorption band depth have drastically reduced from 89% transmittance (11% absorbance) to 96% transmittance (4% absorbance) in the IR spectrum after ARS treatment. This indicates that the $-\text{OH}$ and $-\text{CH}$ functional sites are masked by the dye molecules and thus absorbance of IR radiations in the region 3500 - 2900 cm^{-1} shows a decreasing effect. Similarly, decrease in the absorption bands depth was observed at other functionalities such as $-\text{NH}$ stretching and $\text{C}=\text{O}$, $\text{C}=\text{C}$, $\text{C}-\text{C}$ and $-\text{NH}$ bending vibration bands. The decrease in absorption bands depths and increase in percent transmission

indicate that $-OH$, $-NH$, $-CH$, $C=O$ and $C=C$ functional groups could be responsible for the adsorption of ARS on the surface of adsorbent.

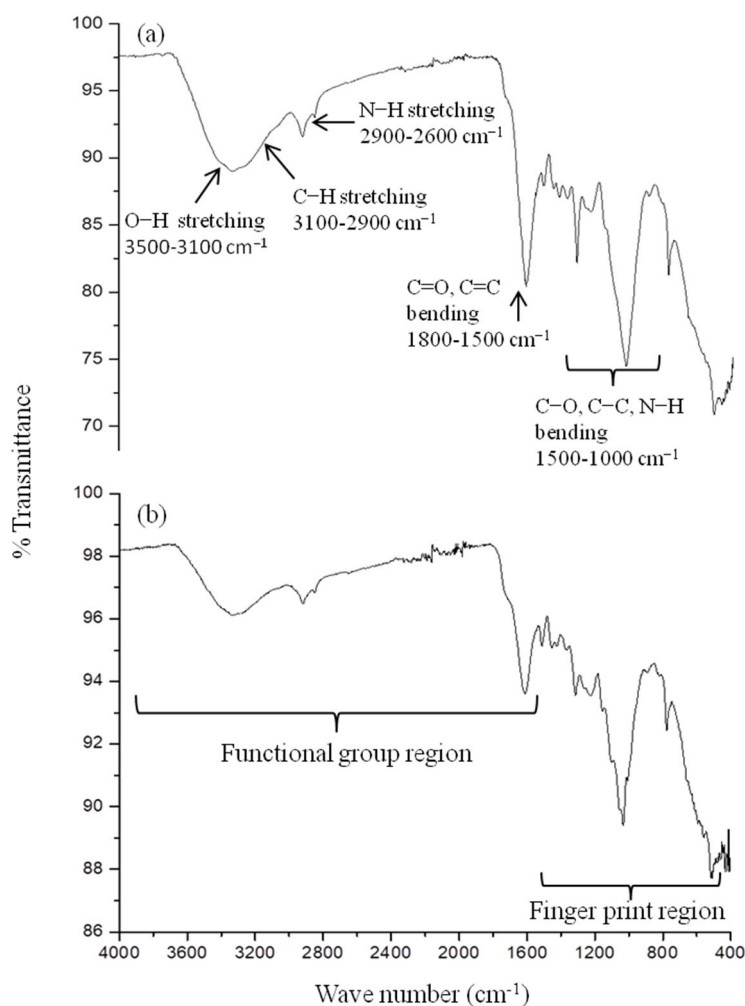


Fig. 2 FTIR spectra of biosorbent (a) before and (b) after loaded with the dye.

Batch adsorption analysis

The influence of Influence of biosorbent dose, contact time, shaking time and temperature on ARS adsorption on to the bark powder of *Ficus religiosa* was examined. The capacity of the dye adsorption of the adsorbent was determined using Eqn. 1, and the results obtained are shown in Figure 3.

The consequences of the biosorbent *Ficus religiosa* dosage on the adsorption of ARS dye was carried out at 0.25, 0.50, 0.75 and 1.00 g per 100 mL of dye at 5, 10, 15 and 20 mg L⁻¹ of the dye solution at 16 hours contact time, 25 °C, shaking time 30 minutes, and at 120 rpm. The results obtained are shown in Fig. 3a from which a high adsorption capacity is observed for low adsorbent dose and maximum adsorption capacity was observed at 0.50 g of the biosorbent. With the increase of the amount of adsorbent beyond 0.50 g, the quantity of adsorption remains almost constant showing that equilibrium is established. Similar behavior was observed by Akaskal *et al.* for malachite green adsorption on loquat seed biomass [45]. It is also evident from Fig. 3a that with a rise in the initial dye concentration, adsorption capacity of the biosorbent increases at each of the amount present in the dye solution. For instance, at 0.25 g of the biosorbent present in the ARS solution, Q_e values at 5, 10, 15 and 20 mg L⁻¹ are 0.341, 0.676, 0.864 and 1.182 mg g⁻¹, respectively. This could be due to multilayer formation on the

biosorbent surface by the ARS dye under the mentioned conditions. A behavior similar to ours for the effect of concentration of ARS dye removal on adsorbent, *Cynodon dactylon* was observed by Samusolomon and Devaprasath [38].

The influence of contact time between biosorbent and adsorbate is an important parameter to study during adsorption processes designed for wastewater treatment systems. The removal of ARS from wastewater was analysed at different lengths of time of contact between ARS and the biosorbent. Figure 3b shows a plot of the adsorption capacity of *Ficus religiosa* for ARS removal from its aqueous solutions at various concentrations versus contact times 8, 16, 24, 32 and 40 hours at optimum conditions (0.50 g of the biosorbent, 30 minutes shaking time and 25 °C). It is evident from Fig. 3b that the capacity of adsorption of the adsorbent for ARS rises with an increase in contact time up to 24 hours and beyond which remain almost constant up to 40 hours of contact time. Thus, maximum adsorption can be achieved at 16 hours as at this time the equilibrium was attained and beyond this time a constant decrease in adsorption capacity was observed. This means that during the first 24 hours all the available sites on the biosorbent were engaged. After that, a cessation of the dye molecules may have occurred that the capacity of adsorption further remain constant [18]. Our results of the effect of contact time on ARS adsorption to biosorbent correspond with literature reporting the adsorption of other dyes on different adsorbents [38, 46, 48-49].

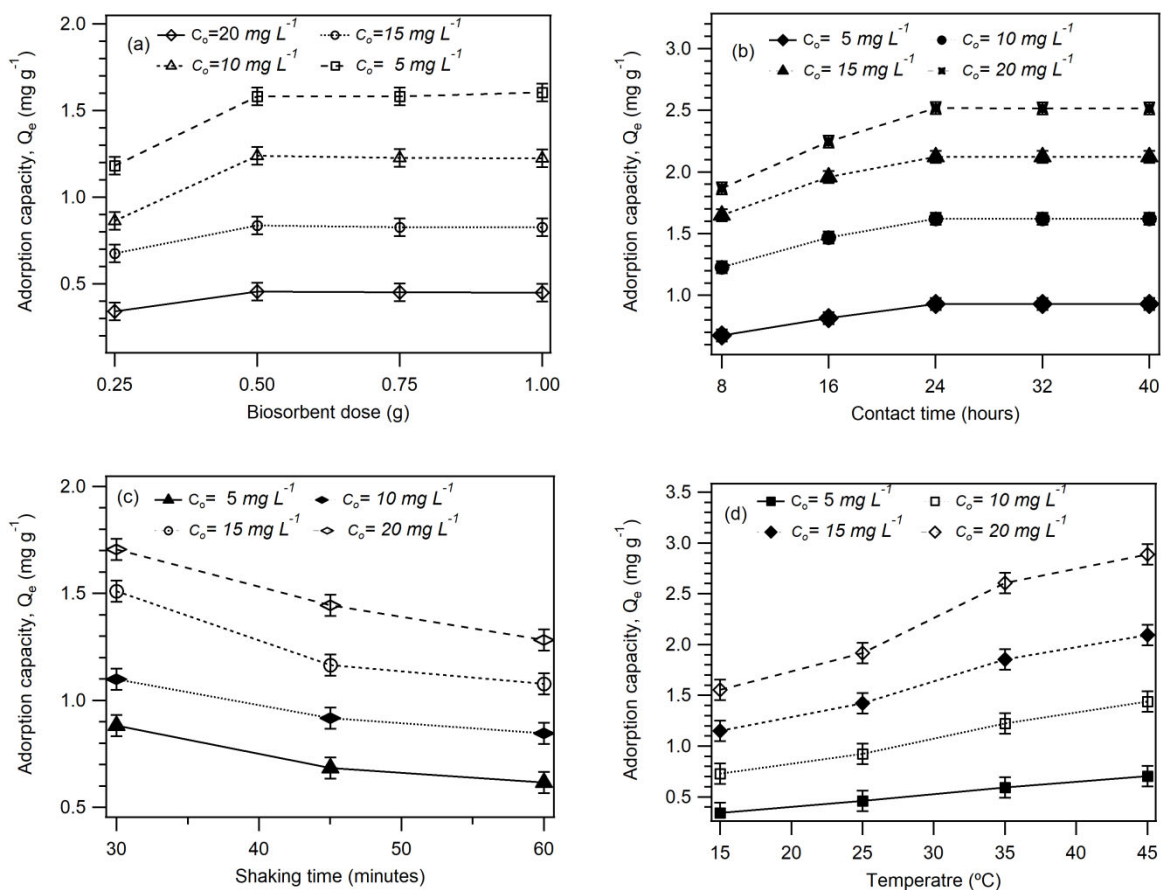


Fig. 3 Plots showing the adsorption capacity of the biosorbent for ARS versus (a) adsorbent dose (b) contact time (c) shaking time and (d) temperature effect at different initial concentrations.

The influence of shaking time on the adsorption of ARS onto *Ficus religiosa* was studied by at the shaking times 30, 45 and 60 minutes at 120 rpm for the flask containing 5, 10, 15 and 20 mg L⁻¹ of ARS dye at other optimum conditions including 0.50 g biosorbent and 25 °C. The results obtained are shown in Fig. 3c which shows that maximum saturation of the adsorptive sites of the biosorbent was reached at a shaking time of 30 minutes for each of the dye concentration. Thus, the optimum shaking time for the biosorption process was 30 minutes as at this time the maximum elimination of ARS dye from wastewater was obtained among all the shaking times studied. At 30 minutes of shaking time, the biosorption process reached equilibrium because a decline in the capacity of adsorption is observed by elevating the shaking time to 45 and then to 60 minutes. This is because when adsorption process reaches equilibrium, the adsorbed dye particles segregate and upon increasing the shaking time they repel more dye particles due to the collision phenomenon [18].

The effect of temperature on the rate of biosorption of ARS dye from aqueous industrial effluents by *Ficus religiosa* bark powder was studied at 0.50 g of adsorbent dose, 24 hours contact time and 32 minutes shaking time in dye solutions of the studied. The temperature of the process was kept at 15, 25, 35 and 45 °C and plotted versus the adsorption capacity obtained at each of these temperatures (Fig. 3d). It is clear from the figure that in each of the initial dye concentrations, at each temperature the capacity of adsorption of the adsorbent increased with a rise in temperature showing that biosorption of ARS onto *Ficus religiosa* bark powder is endothermic in nature. The increase in adsorption at high temperature show a strong interaction at a high speed of the dye molecules with the active sites on the biosorbent material [38].

Adsorption isotherms

The equilibrium data obtained during our study was applied to check various adsorption isotherms to see how the ARS adsorbate interacts with the biosorbent used in the study for designing an adsorption system. An adsorption isotherm relates the quantity of adsorbate (g) adsorbed onto the adsorbent (g) at a given temperature. The three isotherm models (Langmuir, Freundlich and Tempkin) equations (Eq. 4, 5 and 6, respectively) were used to fit our experimental data for obtaining information about the nature of the adsorption of ARS onto our biosorbent, *Ficus religiosa* bark powder. Figure 4 shows linear plots of (a) $1/Q_e$ vs. $1/C_e$ representing Langmuir isotherm, (b) Q_e vs. $\log C_e$ representing Freundlich isotherm and (c) $\log C_e$ vs. Q_e representing Tempkin isotherm, respectively. The parameters for all the isotherms described in equations 2, 3 and 4 were evaluated at 25 °C and 45 °C using slope and intercepts of the plots are illustrated in Table 1.

Langmuir isotherm shows monolayer adsorption with a finite capacity of adsorbate molecules onto the homogeneous, energetically equivalent and identical sites on adsorbent surface. For the $1/Q_e$ vs. $1/C_e$ plot (Fig. 4a) the slope is $1/K_L Q_{max}$. and intercept $1/Q_{max}$. from which Langmuir constants, Q_m and K_L were determined. The Freundlich isotherm model gives information about heterogeneous surfaces and non-uniform enthalpy changes for surface sorption. From the slope and intercept of the $\log q_e$ vs. $\log C_e$ (Fig. 4b), K_F and n values were determined at 25 and 45 °C and are given in Table 1 along with R^2 values.

To get information about uniformity of the distribution of bonding energy, decrease of the enthalpy of adsorption during coverage of all surface sites by adsorbate molecules and indirect interaction between the adsorbate and adsorbent, Tempkin model is employed [45]. Linear equation (Eq. 4) was also applied for fitting Tempkin isotherm model to our data and obtained Tempkin constants K_T and b_T from the plot (Fig. 4c) and are presented in Table 1 along with determination co-efficient at each of the temperatures.

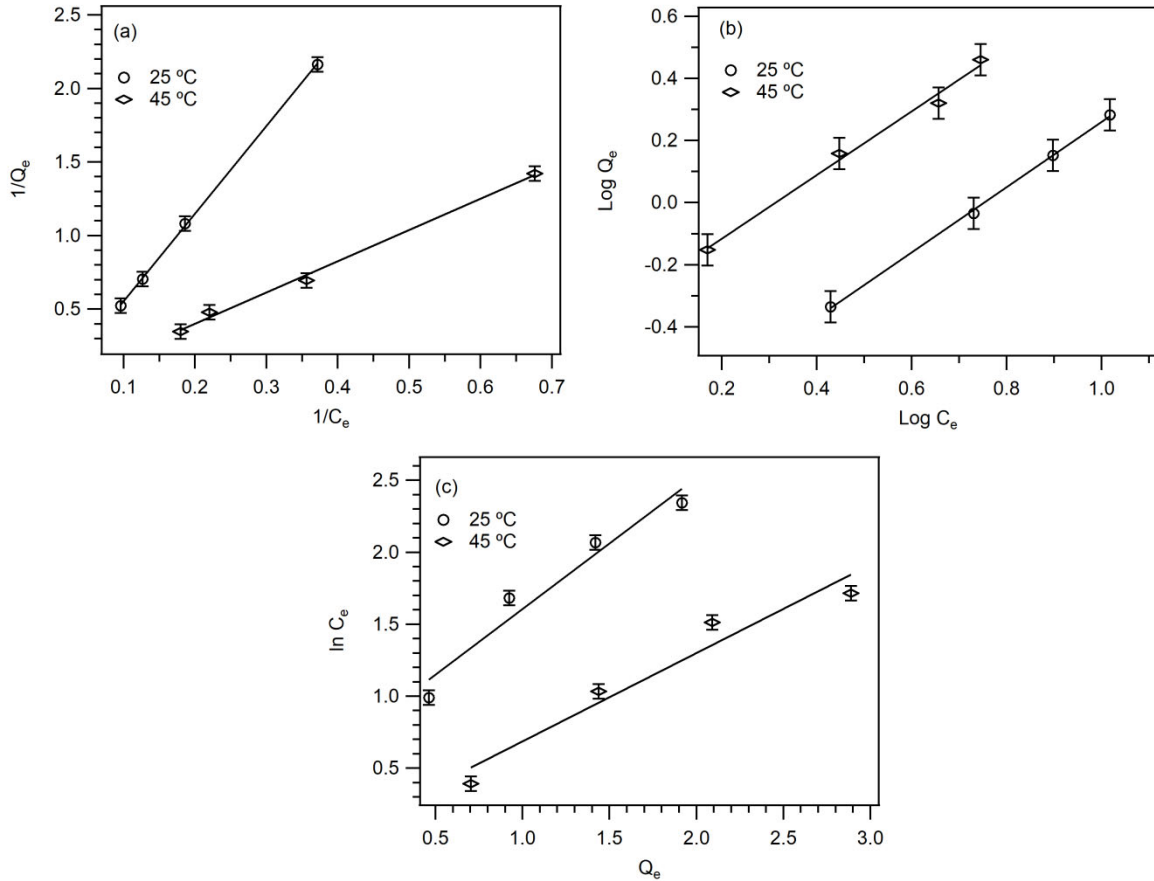


Fig. 4 Adsorption isotherms (a) Langmuir, (b) Freundlich (c) Tempkin of ARS dye by bark powder of *Ficus religiosa* at 25 and 45 °C (Adsorbent dose = 0.50 g, shaking time = 30 minutes and contact time = 24 hours).

The Q_{\max} obtained is 23.81 mg g^{-1} at 25 °C and increased to 38.3 mg g^{-1} at 45 °C showing the preference of high temperature for biosorption of ARS onto the biosorbent. The higher correlation coefficients, R^2 of 0.9997 at 25 °C and 0.9959 at 45 °C shows a best fitted Langmuir isotherm to the equilibrium data. The Freundlich isotherms obtained at different temperatures shows that the parameter K_F and n_F increased with an increase in temperature. The Freundlich exponent (n) value indicates favorable biosorption. Furthermore, high R^2 values 0.9993 and 0.9915 at 25 °C and 45 °C respectively also show that data obey Freundlich isotherm well. Table 1 values show that the Temkin constants K_T and b_T both decreases with an increase in temperature and the regression coefficient obtained at both the temperature are very low 0.9491 (at 25 °C) and 0.9426 (at 45 °C) and the data do not give a good statistical fit of the Temkin model compared to Freundlich and Langmuir models.

Table 1 Langmuir, Freundlich and Temkin adsorption isotherms constants for ARS biosorption on *Ficus religiosa* bark powder.

T (°C)	Langmuir			Freundlich			Temkin		
	Q_{\max}	K_L	R^2	N	K_F	R^2	K_T	b_T	R^2
25	23.81	0.2497	0.9997	0.952	0.162	0.9993	0.9123	0.6934	0.9491
45	38.31	0.0555	0.9959	0.975	0.476	0.9915	0.6143	0.0693	0.9426

Kinetic behavior of adsorption process

The experimental data obtained for ARS adsorption on the biosorbent was applied and fitted in the equations (Eqn. 2 and Eqn. 3) of the two kinetic models and presented in Fig. 6a and 6b, respectively. The best fit kinetic model of the two was chosen based on R^2 and values of the rate constants k_1 and k_2 . Fig. 5a show $\log(Q_e - Q_t)$ versus t plot from which theoretical Q_e value (0.7635 mg g^{-1}) from the slope and k_1 (0.0034545) from the intercept were calculated. The R^2 for first order model is 0.989.

The data was also tested in the pseudo 2nd order kinetic Eqn. 3 and plotted as t/Q_t vs. t and depicted in Fig. 5b. A good statistical fit for the data is obtained with the R^2 (0.999) close to the ideal value ($R^2=1$). The rate constant k_2 is 0.073 higher than the rate constant for the pseudo 1st order rate equation. Thus our data for the ARS adsorption onto *Ficus religiosa* bark powder from aqueous solutions adsorbent follows the 2nd order kinetics predicting that the biosorption rate is not limited by mass transport and may be limited by chemical reaction [40]. A similar pseudo second order fitted data for ARS adsorption onto activated carbon is reported by Ghaedi et al. [45].

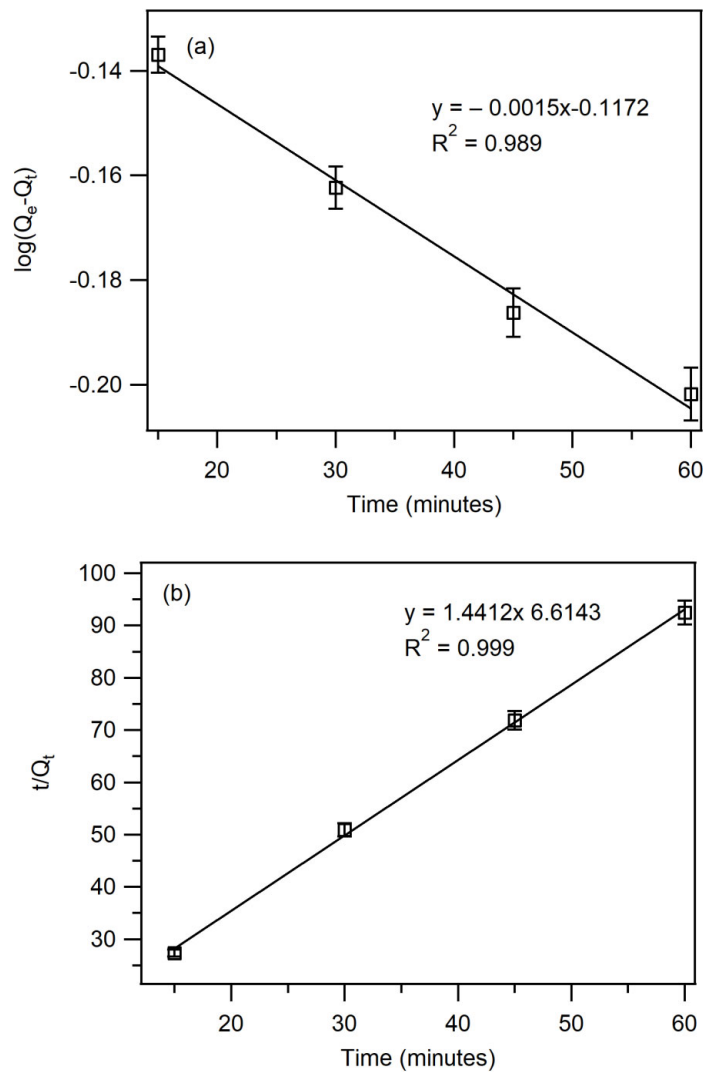


Fig. 5 The kinetics of the ARS removal by the *Ficus religiosa* biosorbent according to (a) pseudo-first order and (b) pseudo-second order model

Conclusion

Ficus religiosa bark powder was first time employed as a productive biosorbent material for the decontamination of ARS dye from industrial aqueous effluents through a viable adsorption method. Scanning electron microscopy analysis of the biosorbent revealed the presence of active binding sites of small particle size with enhanced surface area and subsequent increased biosorption process. The study of FTIR spectra of biosorbent revealed that functional groups responsible for the adsorption of ARS onto the biosorbent were –OH, –NH, –CH, C=O and C=C. The contact time of 24 hours, 0.50 g biosorbent dose, shaking time of 30 minutes and 25 °C were found to be the optimum condition for adsorption of ARS onto the biosorbent. From the kinetic modeling of the biosorption mechanism of the ARS onto *Ficus religiosa* bark powder, the best-fitted kinetic model was the pseudo-2nd order and not the 1st order as evident from the higher R² value. For knowing the mechanism of adsorption, three isotherm models (Langmuir model, Freundlich model and Tempkin model) were tested and the data was best fitted in both Langmuir and Freundlich isotherms compared to Tempkin model. The use of *Ficus religiosa* as a potential biosorbent for the ARS dye removal from wastewater is indeed a fast, eco-friendly and cost-effective approach and can probably be used for the removal of other toxic dyes from water. This research will not only improve the existing techniques of adsorption but will also benefit the researcher who are looking for cost-effective, eco-friendly toxic dye removal substances.

Acknowledgement

The Ammara Gul is highly thankful to the Islamia College Peshawar for providing laboratory facilities for this research work.

Declarations

Funding: The author(s) received no specific funding for this project.

Conflict of Interest: The authors declare that they have no conflict of interest.

Availability of data and material: The authors confirm that the summary of data supporting the findings of this study is available within the article. However, detailed data of this study is available from the corresponding author upon request.

Code availability: Not applicable

References

1. M. Abbas, Experimental investigation of activated carbon prepared from apricot stones material (ASM) adsorbent for removal of malachite green (MG) from aqueous solution, *Adsorp Sci & Technol*, **38**, 24 (2020).
2. Q. Wang and Z. Yang, Industrial water pollution, water environment treatment, and health risks in China. *Environ. Pollut.*, **218**, 358 (2016).
3. A. Azizullah, M.N.K. Khattak, P. Richter, and D.P. Häder, Water pollution in Pakistan and its impact on public health - a review. *Environ. Int.*, **37**, 479 (2011).
4. D. A. Yaseen and Scholz, M., Textile dye wastewater characteristics and constituents of synthetic effluents: a critical review. *Int. Environ. Sci. Technol.*, **16**, 1193 (2019).

5. B. Lellis, C. Z. Fávaro-Polonio, J. A. Pamphile, J. C. Polonio, Effects of textile dyes on health and the environment and bioremediation potential of living organisms. *Biotechnol. Res. Inno.*, **3**, 275 (2019).
6. W. Li, B. Mu and Y. Yang, Feasibility of industrial-scale treatment of dye wastewater via bio-adsorption technology. *Bioresour. Technol.*, **277**, 157 (2019).
7. S.K. Kansal, R. Lamba, S.K. Mehta and A. Umar, Photocatalytic degradation of Alizarin Red S using simply synthesized ZnO nanoparticles. *Mater. Lett.*, **106**, 385 (2013).
8. S. Khan and A. Malik, Toxicity evaluation of textile effluents and role of native soil bacterium in biodegradation of a textile dye. *Environ. Sci. Pollut. Res. - Inter.*, **25**, 4446 (2018).
9. S. Mani and R. N. Bharagava, Exposure to crystal violet, its toxic, genotoxic and carcinogenic effects on environment and its degradation and detoxification for environmental safety. In: de Voogt W. (eds.), *Rev. Environ. Contam. T.*, **237**, Cham: Springer (2016).
10. M.T. Vakili, B. Salamatinia, A.Z. Abdullah, M.H., Ibrahim, K.B. Tan, Z. Gholami and P. Amouzgar, Application of chitosan and its derivatives as adsorbents for dye removal from water and wastewater: A review. *Carbohydr. Polym.*, **113**, 115 (2014).
11. J. Sun, H. Lu, L. Du, H. Lin and H.D. Li, Anodic oxidation of anthraquinone dye Alizarin Red S at Ti/BDD electrodes. *Appl. Surf. Sci.*, **257**, 6667 (2011).
12. A. Dar, A. Safdar and J. Anwar, Removal of anionic dye from industrial effluents with raw and chemically modified chickpea husk. *J. Chem. Soc. Pak.*, **40**, 319 (2018).
13. M.A. Khosa, S.S. Shah and M.F. Nazar, UV-visible spectrometric study and micellar enhanced ultrafiltration of Alizarin Red S dye. *J. Dispers. Sci. Technol.*, **32**, 1634 (2011).
14. B.L. Cíntia, Z.F. Polonio, J.A. Pamphile and J.C. Polonio, Effects of textile dyes on health and the environment and bioremediation potential of living organisms. *Biotechnol. Res. Innov.*, **3**, 275 (2019).
15. J. Gao, J. Yu, Q. Lu, X. He, W. Yang, Y. Li, L. Pu and Z. Yang, Decoloration of Alizarin Red S in aqueous solution by glow discharge electrolysis. *Dyes and Pigms.*, **76**, 47 (2008).
16. C. Novotny, N. Dias, A. Kapanen, K. Malachova, M. Vandrovcova, M. Itavaara and N. Lima, Comparative use of bacterial, algal and protozoan tests to study toxicity of azo-and anthraquinone dyes. *Chemosphere*, **63**, 1436 (2006).
17. L. Laasri, M.K. Elamrani and O. Cherkaoui, Removal of two cationic dyes from a textile effluent by filtration-adsorption on wood sawdust. *Environ. Sci. Pollut. Res.*, **14**, 237 (2007).
18. S. Karcher, A. Kornmüller and M. Jekel, Anion exchange resins for removal of reactive dyes from textile wastewaters. *Water Res.*, **36**, 4717 (2002).
19. A. Szyguła, E. Guibal, M.A. Palacin, M. Ruiz and A.M. Satre, Removal of an anionic dye (Acid Blue 92) by coagulation–flocculation using chitosan. *J. Environ. Manag.*, **90**, 2979 (2009).
20. Y. Sun, G. Wang, Q. Dong, B. Qian, Y. Meng and J. Qiu, Electrolysis removal of methyl orange dye from water by electrospun activated carbon fibers modified with carbon nanotubes. *Chem. Eng. J.*, **253**, 73 (2014).
21. M.F. Abid, M.A. Zablouk and A.M. Abid-Alameer, Experimental study of dye removal from industrial wastewater by membrane technologies of reverse osmosis and nanofiltration. *J. Environ. Health Sci. Eng.*, **9**, 1 (2012).

22. R. Mehrkhah, E. K.Goharshadi, M. M. Ghafurian, M. Mohammadi, O. Mahian, Clean water production by non-noble metal/reduced graphene oxide nanocomposite coated on wood: Scalable interfacial solar steam generation and heavy metal sorption, *J. Sol. Energy*, **224**, 440 (2021).
23. R. Mehrkhah, E. K.Goharshadi, M. Mohammadi, Highly efficient solar desalination and wastewater treatment by economical wood-based double-layer photo absorbers, *J Ind Eng Chem*, **101**, 334-347, (2021).
24. M. Taie, A.Fadaei, M. Sadeghi, S. Hemati, and G. Mardani, Comparison of the Efficiency of Ultraviolet/Zinc Oxide (UV/ZnO) and Ozone/Zinc Oxide (O₃/ZnO) Techniques as Advanced Oxidation Processes in the Removal of Trimethoprim from Aqueous Solutions, *Int. J. Chem. Eng.*, **2021**, Article ID 9640918, 11 (2021). <https://doi.org/10.1155/2021/9640918>
25. K. Kadirvelu, M. Kavipriya, C. Karthika, M. Radhika, N. Vennilamani and S. Patabhi, Utilization of various agricultural wastes for activated carbon preparation and application for the removal of dyes and metal ions from aqueous solutions. *Bioresour. Technol.*, **87**, 129 (2003).
26. M. A. Farajzadeh, S. Pezhhanfar, M. Zarei and A. Mohebbi, Simultaneous elimination of diethyl phthalate, butylated hydroxy toluene and butylated hydroxy anisole from aqueous medium by an adsorption process on pretreated waste material; investigation of isotherms and neural network modeling. *J. Iran. Chem. Soc.* **17**, 1377–1386 (2020).
27. G. Mohammadnezhad and A. K. Behbahan, Polymer matrix nanocomposites for heavy metal adsorption: a review *J. Iran. Chem. Soc.* **17**, 1259–1281, (2020).
28. X. Liu and D.J. Lee, Thermodynamic parameters for adsorption equilibrium of heavy metals and dyes from wastewaters. *Bioresour. Technol.*, **160**, 24 (2014).
29. Ali and V. Gupta, Advances in water treatment by adsorption technology. *Nat. Protoc.*, **1**, 2661 (2006).
30. M. Pipiska, M. Valica, D. Partelova, M. Hornik, J. Lesny and S. Hostin, Removal of synthetic dyes by dried biomass of freshwater moss vesicularia dubyana: a batch biosorption study. *Envir.*, **5**, 1 (2018).
31. E. Rosales, J. Meijide, T. Tavares, M. Pazos and M.A. Sanroman, Grapefruit peelings as a promising biosorbent for the removal of leather dyes and hexavalent chromium. *Process Saf. Environ. Protect.*, **101**, 61 (2016).
32. S. Shakoor and A. Nasar, Adsorptive treatment of hazardous methylene blue dye from artificially contaminated water using cucumis sativus peel waste as a low-cost adsorbent. *Groundw. Sustain. Dev.*, **5**, 152 (2017).
33. S. Subramani and N. Thinakaran, Isotherm, kinetic and thermodynamic studies on the adsorption behaviour of textile dyes onto chitosan. *Process Saf. Environ. Protect.*, **106**, 1 (2017).
34. L.Y. Lee, S.G.M. Siaw, Y. Tan, S.S. Lim, X.J. Lee and Y.F. Lam, Effective removal of Acid Blue 113 dye using overripe Cucumis sativus peel as an eco-friendly biosorbent from agricultural residue. *J. Clean. Prod.*, **113**, 194 (2016).
35. K.S. Rao, S. Anand and P. Venkateswarlu, Adsorption of cadmium from aqueous solution by Ficus religiosa leaf powder and characterization of loaded biosorbent. *Clean-Soil, Air, Water*, **39**, 384 (2011).
36. M. Gregory, B. Divya, R.A. Mary, M. M. H. Viji, V.K. Kalaichelvan and V. Palanivel, Anti-ulcer activity of *Ficus religiosa* leaf ethanolic extract. *Asian Pac. J. Trop. Biomed.*, **3**, 554 (2013).

37. R.K. Gautam, A. Mudhoo and M.C. Chattopadhyaya, Kinetic, equilibrium, thermodynamic studies and spectroscopic analysis of Alizarin Red S removal by adsorption onto mustard husk. *J. Environ. Chem. Eng.*, **1**, 1283 (2013).
38. J. Samusolomon and P.M. Devaprasath, Removal of Alizarin Red S (dye) from aqueous media by using cynodon dactylon as an adsorbent. *J. Chem. Pharm. Res.*, **3**, 478 (2011).
39. R.K. Gautam, P.K. Gautam, M.C. Chattopadhyaya and J.D. Pandey, Adsorption of Alizarin Red S onto biosorbent of Lantana camara: kinetic, equilibrium modeling and thermodynamic studies. *Proceedings of the National Academy of Sciences, India Section A: Phys. Sci.*, **84**, 495 (2014).
40. M. Ishaq, K. Saeed, A. Shoukat, I. Ahmad and A. Rahman, Adsorption of Alizarin Red dye from aqueous solution on an activated charcoal. *Int. J. Sci. Invent. Today*, **3**, 705 (2014).
41. J. I. Goldstein, D. E. Newbury, P. Echlin, D.C. Joy, C. E. Lyman, E. Lifshin, L. Sawyer and J. R. Michael, *Scanning electron microscopy and X-ray microanalysis*. New York: Springer(2017).
42. L. D. Hanke, *Handbook of analytical methods for materials*. Plymouth: Materials Evaluation and Engineering Inc. (2001).
43. A. H. Jawad and A. S. Abdulhameed, Mesoporous Iraqi red kaolin clay as an efficient adsorbent for methylene blue dye: Adsorption kinetic, isotherm and mechanism study, *Surf. Interf.*, **18**, 100422 (2020).
44. A. Malik, K. Abbas, A. Natasha and M.A. Naeem, Comparative study of the adsorption of congo red dye on rice husk, rice husk char and chemically modified rice husk char from aqueous media. *Bull. Chem. Soc. Ethiop.*, **34**, 41 (2020).
45. M. Ghaedi, A. Najibi, H. Hossainian, A. Shokrollahi and M. Soylak, Kinetic and equilibrium study of Alizarin Red S removal by activated carbon. *Toxicol. Environ. Chem.*, **94**, 40 (2012).
46. O. Aksakal, H. Ucun and Y. Kaya, Application of Eriobotrya japonica (Thunb.) Lindley (Loquat) seed biomass as a new biosorbent for the removal of malachite green from aqueous solution. *Water Sci. Technol.*, **59**, 1631 (2009).
47. Y. Liu and Y.J. Liu, Biosorption isotherms, kinetics and thermodynamics. *Sep. Purif. Technol.*, **61**, 229 (2008).
48. F. Cicek, D. Ozer, A. Ozer and A. Ozer, Low cost removal of reactive dyes using wheat bran. *J. Hazard. Mater.*, **146**, 408 (2007).
49. M.C. Ncibi, B. Mahjoub and M. Seffen, Investigation of the sorption mechanisms of metal-complexed dye onto Posidonia oceanica (L.) fibres through kinetic modelling analysis. *Bioresour. Technol.*, **99**, 5582 (2008).